Power-Efficient Multi-User Dual-Function Radar-Communications

Ammar Ahmed, Yujie Gu, Dennis Silage, Yimin D. Zhang
Department of Electrical and Computer Engineering, Temple University, Philadelphia, PA 19122, USA

***Abstract*—Dual-function radar-communication (DFRC) systems have emerged as a promising solution for spectrum sharing in recent years. In this paper, we propose a novel DFRC strategy by exploiting directional power control and waveform diversity. The proposed technique ensures the highest possible magnitude of the radar main beam, resulting in an improved signal-to-noise ratio for the radar operation. This maximization objective is achieved while considering the pre-allocated or adjustable transmit energy requirement for radar and communication operations. The secondary communication objective enabling multi-user access is realized by transmitting distinct amplitude levels and phases towards different communication receivers located in the sidelobe region of the radar. As an example, power allocation for different orthogonal frequency-division multiplexing (OFDM) subcarriers projected towards the radar main beam and the communication receivers is discussed by considering the frequency response of target returns. Simulation results illustrate the performance of the proposed technique.**

***Keywords:* Directional power control, dual-function radar-communications, power allocation, spectrum sharing, waveform diversity**

I. INTRODUCTION

Spectrum sharing has attracted significant research attention in the past few years due to rapidly escalating demand of spectral resources [1]. Increased data rates in wireless communication systems require the expansion of the existing spectrum allocations. Additionally, emerging scientific advances benefiting consumers demand new frequency allocations to fulfill their spectral needs [2]. To effectively manage the existing spectral allocations, several efforts have been made in the area of cognitive radio [3]. Recently, the co-existence of multiple platforms within the same frequency bands has been developed to significantly reduce the spectral congestion by simultaneously sharing the same spectral resources for multiple applications [4, 5]. In this context, the co-existence of radar and communication platforms in the same frequency bands requires both systems to work collaboratively so as to mitigate the mutual interference [6]. Moreover, dual-function radar-communication (DFRC) strategies enabling joint transmission of communication and radar waveforms perform the secondary communication operation in addition to the primary radar function utilizing the same spectral resources [7–13].

The basic principle of a DFRC system is to transmit the waveforms for radar and communication objectives using the same physical platform as illustrated in Fig. 1. A secondary communication function is realized by embedding the communication information in the radar waveforms such that the radar performance is not compromised. The prominent DFRC strategies include waveform diversity-based method [7], sidelobe amplitude modulation (AM) method [8], multi-waveform amplitude shift keying (ASK) method [9], phase shift keying (PSK) method [10], generalized ASK-based method [12], and quadrature amplitude modulation (QAM) method [13].

In the waveform diversity-based DFRC strategy [7], a dictionary of radar waveforms is used such that each waveform corresponds to a unique communication symbol. During a radar pulse, communication objective is realized by selecting the radar waveform corresponding to the desired communication symbol. The sidelobe AM-based method [8] exploits multiple beamforming weight vectors to project different amplitude levels towards the communication receivers located in the sidelobe region of the radar. Each sidelobe level represents unique communication information. In the multi-waveform ASK-based method [9], each radar waveform is associated with a beamforming weight vector implementing different sidelobe control-based information embedding. The communication receivers decode the transmitted waveform and the corresponding sidelobe level to determine the transmitted information. A generalized mathematical framework for multi-waveform ASK-based DFRC techniques was introduced in [12]. This method enables multi-user access by projecting radar waveforms with different sidelobe levels towards the communication receivers located in different directions. In the PSK-based information embedding strategy [10], a dictionary of beamforming weight vectors is exploited such that each beamforming vector results in a different phase delay towards the communication receivers. This PSK-based information for the multiple transmitted waveforms can be decoded by the communication receivers using matched filtering. The QAM-based information embedding strategy [13] provides a DFRC solution to realize multi-user access by projecting the radar waveforms with distinct sidelobe levels and phases in different directions. The QAM-based method also serves as a generalized mathematical framework for the existing sidelobe control-based DFRC techniques [8–13].

In this paper, we propose a novel DFRC strategy to ensure maximum transmit power in the radar main beam while

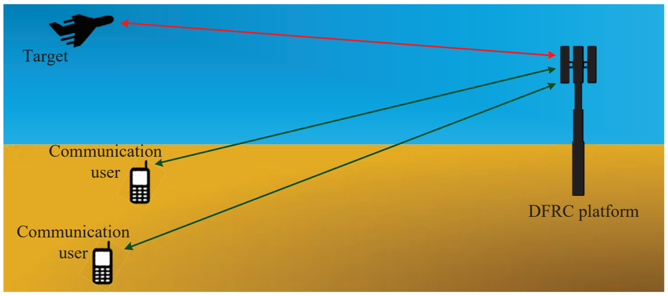

Fig. 1.   The basic principal of dual-function radar-communications system.

exploiting directional power control and waveform diversity. The primary radar objective is achieved without compromising the communication of information to the users located in the sidelobe region of radar. Unlike the conventional DFRC schemes which transmit equal power in all the radar waveforms [8–13], the proposed method is able to control the transmit power for each waveform towards radar and communication directions depending on the target reflections. Optimized power allocation results in the highest signal-to-noise ratio (SNR) at the radar receiver to improve target detection. The proposed approach enables multi-user access by transmitting distinct communication symbols in different directions while exploiting the same hardware resources as used by the existing methods [8–13]. Therefore, the proposed DFRC strategy provides much greater flexibility in system design compared to existing methods. Simulation results demonstrate the effectiveness of the proposed DFRC method.

II. SYSTEM MODEL

Consider a DFRC system consisting of M linear transmit array elements arranged in an arbitrary fashion. The primary function of the DFRC system is to ensure the unperturbed radar operation while performing a secondary communication activity. The objective of the radar operation is to maintain a desired magnitude of the radar signal towards the radar main lobe. Moreover, the DFRC system provides communication information to R users located in the sidelobe region of the radar in different directions. Denote P_{total} as the total power transmitted by the antenna array and $\psi_1(t), \psi_2(t), \ldots, \psi_{\hat{K}}(t)$ as the $\hat{K}$ mutually orthogonal waveforms which are available to the DFRC system. Here, t is the fast time and each waveform $\psi_k(t)$ $(1 \leq k \leq \hat{K})$ is normalized to unit average power such that:

$$\frac{1}{T_p}\int_0^{T_p} \psi_{k_1}(t)\,\psi_{k_2}(t)dt = \delta(k_1 - k_2), \quad 1 \leq k_1, k_2 \leq \hat{K}, \tag{1}$$

where T_p denotes the radar pulse period. To realize the objectives of the DFRC system, different beamforming weight vectors are synthesized to enable multiple information streams towards the communication receivers while keeping the radar main beam at a constant amplitude. The following optimization problem is formulated for this purpose [8–13]:

$$\begin{aligned} \min_{\mathbf{u}_n} \max_{\theta_i} & \left| G e^{j\varphi(\theta_i)} - \mathbf{u}_n^{\text{H}} \mathbf{a}(\theta_i) \right|, && \theta_i \in \Theta_{\text{rad}}, \\ \text{subject to } & \left| \mathbf{u}_n^{\text{H}} \mathbf{a}(\theta_p) \right| \leq \varepsilon, && \theta_p \in \Theta_{\text{sll}}, \\ & \mathbf{u}_n^{\text{H}} \mathbf{a}(\theta_r) = \Delta(\theta_r) e^{j\phi(\theta_r)}, && \theta_r \in \Theta_{\text{com}}, \end{aligned} \tag{2}$$

where Θ_{rad} denotes the directions at which the radar main beam operates, Θ_{com} contains the directions of communication receivers located in the sidelobe region of radar, and Θ_{sll} denotes the complement set of $\Theta_{\text{rad}} \cup \Theta_{\text{com}}$ representing the remaining sidelobe region. In addition, $\mathbf{a}(\theta)$ is the array manifold vector of the transmit antenna array at angle θ, G is the desired magnitude of radar main lobe, $\varphi(\theta)$ is the desired phase profile of radar at angle θ, and $(.)^{\text{H}}$ represents the Hermitian operator. Further, $\mathbf{u}_n$ is the desired beamforming weight vector which achieves the sidelobe level $\Delta(\theta_r)$ with phase $\phi(\theta_r)$ at the communication receiver located at an angle θ_r $(1 \leq r \leq R)$. Each pair of $\Delta(\theta_r)$ and $\phi(\theta_r)$ can take any of the L possible sidelobe levels and Q allowable phase symbols, respectively, towards angle θ_r. Moreover, $\mathbf{u}_n$ guarantees a sidelobe level having a maximum value of ε in the sidelobe region if $\Delta(\theta_r) \leq \varepsilon$ for $1 \leq r \leq R$.

The transmitted signal from the DFRC system can be expressed as:

$$\mathbf{s}(t,\tau) = \sqrt{\frac{P_{\text{total}}}{K}} \sum_{k=1}^{K} \mathbf{U}\mathbf{b}_k(\tau)\psi_k(t), \tag{3}$$

where τ is the slow time, and $\mathbf{U} = [\mathbf{u}_1^*, \mathbf{u}_2^*, \cdots, \mathbf{u}_N^*]$ is an $M \times N$ dictionary matrix which includes N beamforming weight vectors synthesized from (2). Each beamforming vector in $\mathbf{U}$ results in a unique set of amplitude levels and phase offsets in the directions of communication receivers while keeping the radar beam at a constant amplitude. Here, $(.)^*$ denotes the conjugate operator. In addition, $\mathbf{b}_k(\tau) = [b_{1,k}(\tau), b_{2,k}(\tau), \cdots, b_{N,k}(\tau)]^{\text{T}}$ is an $N \times 1$ selection vector which chooses the desired beamforming weight vector $\mathbf{u}_k$ from the dictionary matrix $\mathbf{U}$ for each transmitted waveform $\psi_k(t)$, where $(.)^{\text{T}}$ denotes the transpose operator. All the elements in $\mathbf{b}_k(\tau)$ are zero except only one element which is equal to 1. We utilize K $(\leq \hat{K})$ orthogonal waveforms during each radar pulse and it is possible to use different values of K for each pulse. From (2), note that the amplitudes and phases of the transmitted waveforms towards communication receivers in different directions can be distinct during each radar pulse. Depending on the choice of N and K, different DFRC schemes [8–13] can be realized.

III. PROPOSED INFORMATION EMBEDDING STRATEGY

We observed that the existing DFRC techniques do not optimize the maximum possible energy which can be transmitted in the direction of radar main beam. Moreover, each waveform $\psi_k(t)$ in the radar pulse is transmitted with an equal power towards the main beam of radar. In practice, it might be desirable to operate the radar main beam at the highest possible amplitude to efficiently detect the weak targets. In addition, modern radars change the power allocation for each transmitted frequency to ensure the best performance when the radar cross-section (RCS) of the target is frequency-dependent [14]. Therefore, it is also important for future DFRC systems to offer power allocation capabilities.

A. Proposed Information Embedding

In our approach, we optimize the amplitude of each radar waveform towards the radar main beam given the RCS-dependent power allocation for each waveform. Fig. 2 shows the basic principle of the proposed method. We generate K $(\leq \hat{K})$ beamforming weight vectors $\mathbf{u}_k$ such that each vector corresponds to one of the available radar waveforms $\psi_k(t)$, where $1 \leq k \leq K$. The signal transmitted from the DFRC platform can be expressed in the following form:

$$\mathbf{s}(t,\tau) = \sum_{k=1}^{K} \mathbf{u}_k^*(\tau)\psi_k(t), \tag{4}$$

where $\mathbf{u}_k(\tau)$ can be changed for each pulse time τ depending on the desired phase and amplitude levels towards the radar beam and the communication users. The beamforming weight

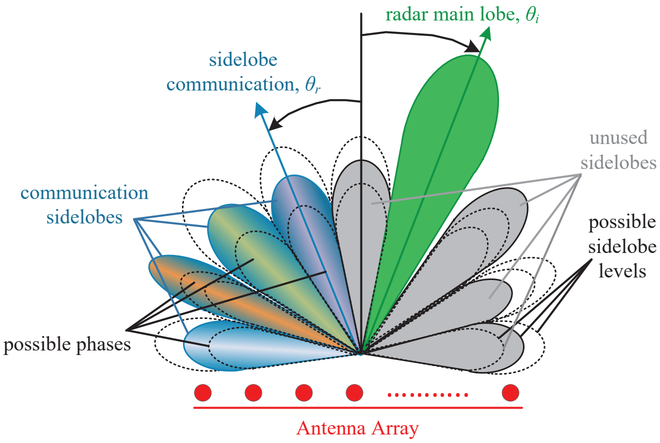

Fig. 2. The proposed DFRC strategy.

vector $\mathbf{u}_k$ can be calculated using the following optimization problem (note that τ is omitted for notational simplicity):

$$\begin{aligned} \max_{\mathbf{u}_k} \quad & G_k \\ \text{subject to} \quad & \left|G_k e^{j\varphi_k(\theta_i)} - \mathbf{u}_k^{\mathrm{H}}\mathbf{a}(\theta_i)\right| = 0, && \theta_i \in \Theta_{\text{rad}}, \\ & \mathbf{u}_k^{\mathrm{H}}\mathbf{a}(\theta_r) = \Delta(\theta_r) e^{j\phi(\theta_r)}, && \theta_r \in \Theta_{\text{com}}, \\ & \left|\mathbf{u}_k^{\mathrm{H}}\mathbf{a}(\theta_p)\right| \leq \varepsilon, && \theta_p \in \Theta_{\text{sll}}, \\ & \sum_{\theta_q} \left|\mathbf{u}_k^{\mathrm{H}}\mathbf{a}(\theta_q)\right|^2 = P_k, && \theta_q \in \Theta_{\text{all}}, \\ & \sum_{\theta_i} \left|\mathbf{u}_k^{\mathrm{H}}\mathbf{a}(\theta_i)\right|^2 = \gamma_k P_k, && \theta_i \in \Theta_{\text{rad}}, \\ & \sum_{\theta_p} \left|\mathbf{u}_k^{\mathrm{H}}\mathbf{a}(\theta_p)\right|^2 = (1-\gamma_k) P_k, && \theta_p \in \bar{\Theta}_{\text{rad}}, \end{aligned} \tag{5}$$

where G_k is the desired amplitude of the transmitted waveform $\psi_k(t)$ in the direction of the radar main beam Θ_{rad}, and P_k denotes the total power available to the DFRC platform for the waveform $\psi_k(t)$. Moreover, γ_k ($\gamma_k \in [0,1]$) and $1-\gamma_k$, respectively, denote the power proportion designated for radar main lobe and radar sidelobe region $\bar{\Theta}_{\text{rad}}$ by the waveform $\psi_k(t)$. In addition, Θ_{all} contains all the angles from -90^{o} to 90^{o} and $\bar{\Theta}_{\text{rad}} = \Theta_{\text{com}} \cup \Theta_{\text{sll}}$ represents the complement set of Θ_{rad}. Note that the proposed approach aims to maximize the transmitted power in the radar main beam while considering the power allocated to radar and communication systems.

Alternatively, the optimization problem in (5) can be relaxed as a convex optimization problem as follows:

$$\begin{aligned} \min_{\mathbf{u}_k} \quad & -G_k \\ \text{subject to} \quad & \left|G_k e^{j\varphi_k(\theta_i)} - \mathbf{u}_k^{\mathrm{H}}\mathbf{a}(\theta_i)\right| \leq \beta_{\text{tol}}, && \theta_i \in \Theta_{\text{rad}}, \\ & \mathbf{u}_k^{\mathrm{H}}\mathbf{a}(\theta_r) = \Delta(\theta_r) e^{j\phi(\theta_r)}, && \theta_r \in \Theta_{\text{com}}, \\ & \left|\mathbf{u}_k^{\mathrm{H}}\mathbf{a}(\theta_p)\right| \leq \varepsilon, && \theta_p \in \Theta_{\text{sll}}, \\ & \left|\mathbf{u}_k^{\mathrm{H}}\mathbf{A}(\Theta_{\text{all}})\right|_2 \leq \sqrt{P_k}, \\ & \left|\mathbf{u}_k^{\mathrm{H}}\mathbf{A}(\Theta_{\text{rad}})\right|_2 \leq \sqrt{\gamma_k P_k}, \\ & \left|\mathbf{u}_k^{\mathrm{H}}\mathbf{A}(\bar{\Theta}_{\text{rad}})\right|_2 \leq \sqrt{(1-\gamma_k) P_k}, \end{aligned} \tag{6}$$

where β_{tol} is the error tolerance for the desired radar beampattern towards the main beam and $\mathbf{A}(\Theta) = [\mathbf{a}(\theta_1), \mathbf{a}(\theta_2), \cdots, \mathbf{a}(\theta_j)]$ with $\{\theta_1, \theta_2, \cdots, \theta_j\} \in \Theta$. From Eqs. (4)-(6), the powers P_{rad} and P_{com} transmitted in the radar main beam and the sidelobe region, respectively, can be expressed as:

$$P_{\text{rad}} \leq \sum_{k=1}^{K} \gamma_k P_k, \quad P_{\text{com}} \leq \sum_{k=1}^{K} (1-\gamma_k) P_k. \tag{7}$$

Thus, the maximum power transmitted from antenna array is $P_{\text{total}} = P_{\text{rad}} + P_{\text{com}}$.

From Eqs. (4) and (6), it can be observed that different radar waveforms can be transmitted with different power levels towards the main lobe. Moreover, we have an added flexibility to maximize the transmitted power towards the radar main beam while ensuring the communication performance. All the tasks are performed within the power constraints for the communications and radar purpose. These power allocations can change with respect to target response and communication environment.

As an example, we can control the maximum transmitted energy of each frequency component for the transmission based on orthogonal frequency-division multiplexing (OFDM) by controlling the power P_k of the corresponding subcarrier $\psi_k(t)$. This can be helpful to enhance the target characterization with frequency-dependent RCS [14]. In this context, a higher SNR can be achieved by maximizing the radar amplitudes in the frequencies where RCS is high (by selecting appropriate P_k and γ_k). This strategy results in an improved SNR for radar receiver, whereas communication users are still entertained with all the desired frequencies by allowing $(1-\gamma_k)P_k$ power towards the radar sidelobe region for all the subcarriers.

B. Detection at the Communication Receiver

The signal received at the r-th communication receiver at the angle θ_r can be expressed as:

$$x_r(t,\tau) = h_r(\tau)\, \mathbf{a}^{\mathrm{T}}(\theta_r)\, \mathbf{s}(t,\tau) + n_r(t), \tag{8}$$

where $h_r(\tau)$ is the channel coefficient summarizing the propagation environment between the transmit array and r-th communication user, and $n_r(t)$ is the zero-mean additive white Gaussian noise. Matched filtering of the received signal $x_r(t,\tau)$ to each of the K $(\leq \hat{K})$ possible waveforms at the r-th communication receiver yields the following scalar:

$$\begin{aligned} y_{r,k}(\tau) &= \frac{1}{T_p} \int_0^{T_p} x_r(t,\tau)\, \psi_k(t)\, dt \\ &= \begin{cases} h_r(\tau)\Delta(\theta_r) e^{j\phi(\theta_r)} + n_{r,k}(\tau), & \text{if } \psi_k(t) \text{ transmitted,} \\ n_{r,k}(\tau), & \text{otherwise,} \end{cases} \end{aligned} \tag{9}$$

where $n_{r,k}(\tau)$ is the noise at the output of k-th matched filter. By analyzing $y_{r,k}(\tau)$ at the r-th communication receiver located in the direction of θ_r, the receiver can determine the respective amplitude and phase to decode the embedded communication information.

C. Sum Data Rate Analysis

We calculate the sum data rate which can be received by the R sidelobe communication users located in unique directions within the sidelobe region of the radar. Considering K orthogonal waveforms, L sidelobe levels, and Q possible phases for each communication user, Eq. (4) can be utilized to determine the information capacity during each radar pulse. It can be observed that $\log_2 LQ$ bits can be transmitted with each radar waveform $\psi_k(t)$ at each communication receiver when L sidelobe levels and Q phases are exploited. This implies that the total number of bits which can be transmitted during each radar pulse is $RK \log_2 LQ$. It is important to note that the information streams transmitted to each communication receiver may or may not be distinct, respectively corresponding to multi-user access and broadcast mode.

IV. SIMULATION RESULTS

We consider a uniform linear array (ULA) consisting of 20 transmit antennas. The primary function of the radar is to form a main beam between -5^o and 5^o. There are $R = 2$ communication receivers located in the sidelobe region at 40^o and 50^o, respectively. For each communication user located at θ_r ($1 \leq r \leq R$), we consider two possible sidelobe levels ($L = 2$) and two different phases ($Q = 2$). These corresponding sidelobe levels $\Delta(\theta_r)$ can either be 0.1 (i.e., -20 dB) or 0.0316 (i.e., -30 dB) at each communication receiver during a radar pulse. Similarly, the projected phases $\phi(\theta_r)$ at each communication receiver can take a value of 0 or π radians. Using Eq. (6), we can generate the beamforming weight vectors which satisfy these specifications. We exploit $K = 1,024$ OFDM subcarriers with a bandwidth of 100 MHz centered at 3 GHz to achieve the DFRC objectives. For the case of equal power transmission through all the OFDM subcarriers (i.e., $P_1 = P_2 = \cdots = P_{1024}$), we design four different beampatterns using Eq. (6) as shown in Fig. 3(a). It can be observed that each beampattern has a unique set of sidelobe levels for the communication users while maintaining the 0 dB amplitude in radar main beam.

Next, we consider two point targets located within the radar main beam at 100.1 km and 101.5 km, respectively, from the DFRC system. The targets are assumed to have a high electromagnetic reflectivity for only 400 OFDM subcarriers clustered at the center of the transmitted bandwidth. This information about RCS can be obtained by calculating the spectrum of the reflected signal at radar receiver. To achieve the optimal SNR for the radar system, the DFRC platform is optimized for the subsequent radar pulses such that more power is allocated to the frequencies with a higher target reflectivity. In this context, Fig. 3(b) shows the respective transmit beampatterns for the subcarriers with low target reflectivity, whereas Fig. 3(c) corresponds to the transmit beampatterns for the highly reflected subcarrier. From Fig. 3(b) and Fig. 3(c), it can be observed that the transmitted energy in the radar main beam varies for different frequencies without deteriorating the communication performance. It is important to note that the magnitude response of all the beampatterns in Fig. 3 remains the same for different phases $\phi(\theta_r)$ towards the communication receivers. Therefore, we have only shown the beampatterns for $\phi(\theta_r) = 0$ at each communication receiver.

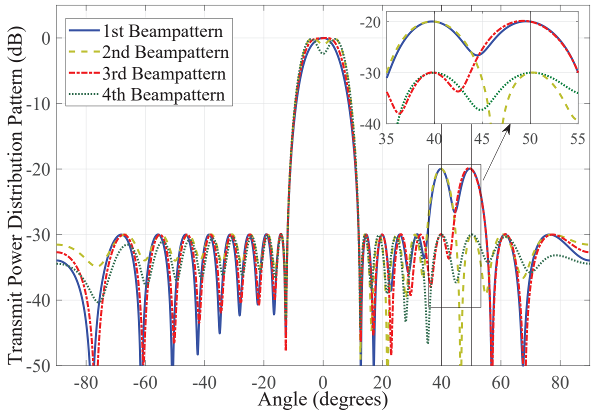

(a) Case I: Beampattern synthesis for equal power in all subcarriers

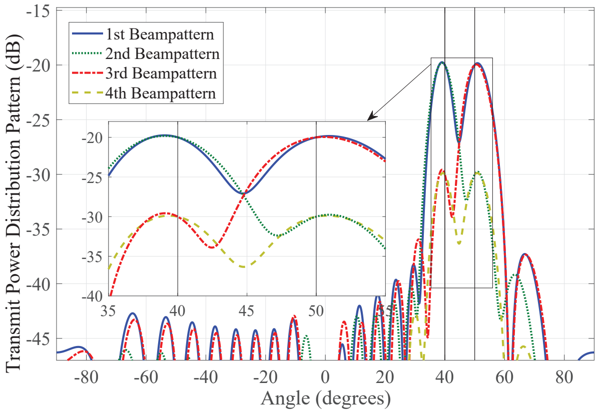

(b) Case II: Beampatterns for subcarriers with low target reflectivity

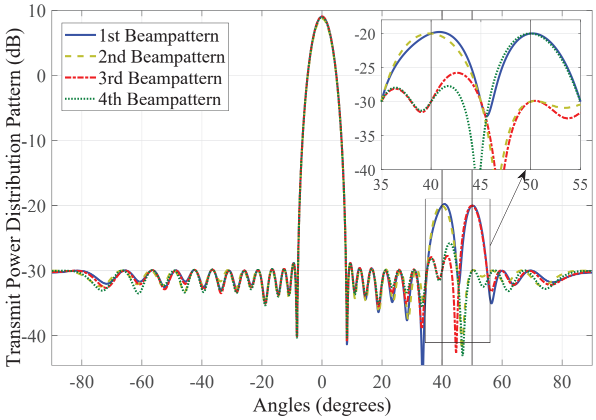

(c) Case II: Beampatterns for subcarriers with high target reflectivity

Fig. 3. Example beampatterns using the proposed approach (ULA with $M = 20$, $R = 2$ communication receivers located at 40^o and 50^o).

In Fig. 4, we present the range estimation and symbol error rate performance for the cases of equal power and optimal SNR. The radar range is estimated using the technique illustrated in [4] by considering a radar range cell from 100 km to 100.3 km. Additive white Gaussian noise of equal power is considered for both cases at the radar receiver. It can be observed from Fig. 4(a) that the optimal SNR provides considerable performance enhancement in range estimation. This is a significant improvement since the total power

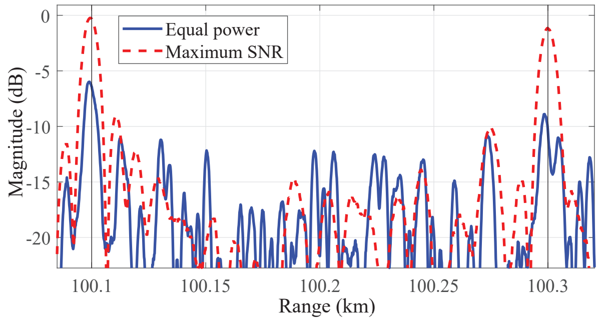

(a) Radar range profile for equal power and max. SNR case

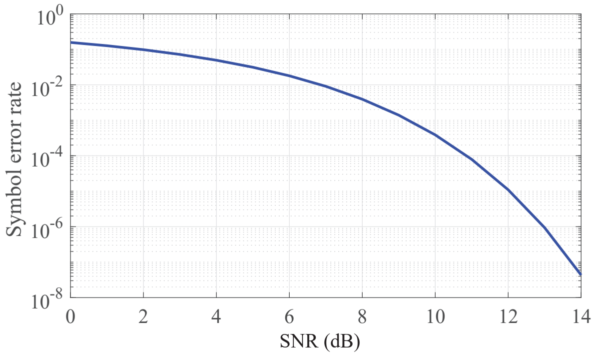

(b) Symbol error rate at the communication receiver

Fig. 4. Range estimation and symbol error rate performance for the proposed technique.

transmitted by the array and the total power projected in the radar main beam are kept constant for both cases. The only difference is the transmitted power for different subcarriers based on the RCS. The proposed approach provides better performance because more power is allocated to the frequencies with a higher target reflectivity.

Communication performance is illustrated in Fig. 4(b) in terms of symbol error rate. We consider coherent QAM-based approach [12] by exploiting two phases and two sidelobe levels for each transmitted OFDM waveform $(L = 2, Q = 2, K = 1,024)$. Note that independent data streams are transmitted to both communication receivers simultaneously. Only one curve is plotted here because the symbol error rates for the case of equal power and optimal SNR are the same. This is because the change in radar main beam does not deteriorate the required signal amplitudes and phases at the communication receivers, which can be observed in Fig. 3. Thus, the improvement in radar range estimation is achieved without compromising the performance of communication system. Thus, the simulation results illustrate the effective performance achieved by the proposed DFRC strategy.

V. CONCLUSION

A novel DFRC strategy was proposed to ensure the maximum SNR in the radar main lobe by optimizing the transmit beampattern. The proposed method allocates the desired power in radar and communication directions for each transmitted waveform based on the RCS. Optimized power allocation results in higher SNR at the radar receivers which enables a better characterization of targets. While ensuring the radar's objectives, the proposed approach transmits distinct amplitudes and phases in different directions enabling the multi-user access. As an example, OFDM subcarriers are used as the radar waveforms for performing DFRC objectives. The power of different subcarriers towards radar main beam was varied by inspecting the target returns while keeping the total transmitted energy constant for radar and communication objectives. The proposed DFRC strategy resulted in improved target detection without any degradation in the performance of communication system.

ACKNOWLEDGEMENT

This work is supported in part by the National Science Foundation (NSF) under grant AST-1547420.

REFERENCES

[1] H. T. Hayvaci and B. Tavli, "Spectrum sharing in radar and wireless communication systems: A review," in *Proc. Int. Conf. Electromagn. in Advanced Appl.*, Palm Beach, Aruba, Aug. 2014, pp. 810–813.

[2] S. Kumar, G. Costa, S. Kant, B. F. Flemming, N. Marchetti, and P. Mogensen, "Spectrum sharing for next generation wireless communication networks," in *Proc. Int. Workshop on Cognitive Radio and Advanced Spectr. Manag.*, Aalborg, Denmark, Feb. 2008, pp. 1–5.

[3] E. Biglieri, *Principles of Cognitive Radio*, Cambridge University Press, 2012.

[4] C. Sturm, T. Zwick, and W. Wiesbeck, "An OFDM system concept for joint radar and communications operations," in *Proc. IEEE Veh. Technol. Conf.*, Barcelona, Spain, Apr. 2009, pp. 1–5.

[5] Z. Geng, H. Deng, and B. Himed, "Adaptive radar beamforming for interference mitigation in radar-wireless spectrum sharing," *IEEE Signal Process. Lett.*, vol. 22, no. 4, pp. 484–488, Apr. 2015.

[6] D. W. Bliss, "Cooperative radar and communications signaling: The estimation and information theory odd couple," in *Proc. IEEE Radar Conf.*, Cincinnati, OH, May 2014, pp. 50–55.

[7] S. D. Blunt, M. R. Cook, and J. Stiles, "Embedding information into radar emissions via waveform implementation," in *Proc. Waveform Diversity and Design Conf.*, Niagara Falls, Canada, Aug. 2010, pp. 195–199.

[8] J. Euziere, R. Guinvarc'h, M. Lesturgie, B. Uguen, and R. Gillard, "Dual function radar communication time-modulated array," in *Proc. Int. Radar Conf.*, Lille, France, Oct. 2014, pp. 1–4.

[9] A. Hassanien, M. G. Amin, Y. D. Zhang, and F. Ahmad, "Dual-function radar-communications: Information embedding using sidelobe control and waveform diversity," *IEEE Trans. Signal Process.*, vol. 64, no. 8, pp. 2168–2181, Apr. 2016.

[10] A. Hassanien, M. G. Amin, Y. D. Zhang, and F. Ahmad, "Phase-modulation based dual-function radar-communications," *IET Radar, Sonar & Navigation*, vol. 10, no. 8, pp. 1411–1421, Oct. 2016.

[11] A. Hassanien, M. G. Amin, Y. D. Zhang, and F. Ahmad, "Signaling strategies for dual-function radar communications: An overview," *IEEE Aerosp. Electron. Syst. Mag.*, vol. 31, no. 10, pp. 36–45, Oct. 2016.

[12] A. Ahmed, Y. D. Zhang, and B. Himed, "Multi-user dual-function radar-communications exploiting sidelobe control and waveform direversity," in *Proc. IEEE Radar Conf.*, Oklahoma City, OK, Apr. 2018.

[13] A. Ahmed, Y. D. Zhang, and Y. Gu, "Dual-function radar-communications using QAM-based sidelobe modulation," *Digital Signal Process.*, (under review).

[14] K. W. Huang, M. Bic, U. Mitra, and V. Koivunen, "Radar waveform design in spectrum sharing environment: coexistence and cognition," in *IEEE Radar Conf.*, Arlington, VA, May 2015, pp. 1698–1703.